



Ab initio calculations of open cell voltage in newly designed PTMA-based Li-ion organic radical batteries



Nicolas Dardenne*, Geoffroy Hautier, Jean-François Gohy, Jean-Christophe Charlier, Gian-Marco Rignanese

Institute of Condensed Matter and Nanoscience (IMCN), Université catholique de Louvain, B-1348 Louvain-la-Neuve, Belgium

ARTICLE INFO

Article history:

Received 4 July 2017

Received in revised form 22 September 2017

Accepted 21 October 2017

Keywords:

DFT
Reduction potential
Solvation
Organic radical
Li-ion

ABSTRACT

In this work, density functional theory is used to predict the voltage of newly designed PTMA-based radical molecules. Organic radical molecules have recently been tested as promising materials for secondary batteries due to their processability and structural diversity. In order to tune the redox potentials, we investigate the substitution of functional groups on the actual TEMPO organic radical. Our first-principles simulations predict voltages ranging between 3.4 and 6.2 V allowing for a fine-tuning of the corresponding voltage for specific needs.

© 2017 Elsevier B.V. All rights reserved.

1. Introduction

Polymers with tunable optical and electronic properties are nowadays the subject of intense research in order to find replacement materials for the current inorganic devices. For batteries, currently available Li-ion cells are based on inorganic materials, such as LiCoO₂, with some issues in terms of cost due to limited natural resources and in terms of waste management due to the toxicity of the constituents [1]. Organic polymers based on renewable resources could provide a way to develop a green battery [2–4]. They also present advantages such as low-cost production and flexibility. Recently, organic radical polymers have attracted a lot of attention due to their potential to be used as cathode in Li-ion batteries. The most studied radical compounds used in organic radical batteries (ORBs) are nitroxide based polymers [5]. Among these, Poly(2,2,6,6-tetramethyl-1-piperidinyloxy-4-yl methacrylate) (PTMA) is the most commonly utilized as cathode in Li-ion ORB (Li-ORB), exhibiting high charging and discharging rates and long cycle-life [6].

To improve the performance of these batteries i.e. to increase the reduction potential or to decrease the molar mass, molecular engineering could be applied to various organic radicals. In a pre-

vious article [7], it was shown that a Δ SCF technique based on density functional theory (DFT) [8,9] calculations associated with the SMD [10] polarizable continuum model can predict the redox potentials of various organic radicals within 0.1 V. Moreover, the method reproduces the shifts in the reduction potential when changing various functional groups for a given molecule.

Using this predictive approach, newly designed radicals are investigated. Starting from the PTMA molecule, the methyl groups around the nitroxide center are substituted with various functional groups in order to study their effects on the redox potential. The voltage are found to range from 3.4 up to 6.2 V depending on the number and the position of the functional groups.

2. The method

The first redox radical polymer used in a Li-ORB was PTMA [a poly(methacrylate) (PMMA) bearing a 2,2,6,6-tetramethyl-1-piperidinyloxy radical (TEMPO)] [11]. This TEMPO radical which is linked to the PMMA backbone (Fig. 1b) presents a nitroxide center with a localized unpaired electron allowing reversible oxidation to form an oxoammonium cation (p-type doping) or reversible reduction to an aminoxyl anion (n-type doping) (Fig. 1c). This characteristic localized unpaired electron is illustrated in Fig. 1a with the computed spin-up density of the radical TEMPO where the SOMO (single occupied molecular orbital) is equally distributed on the nitroxide center.

* Corresponding author.

E-mail addresses: n.dardenne@uclouvain.be (N. Dardenne), gian-marco.rignanese@uclouvain.be (G.-M. Rignanese).

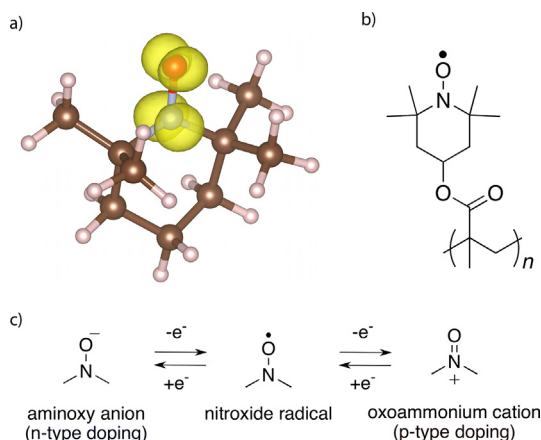
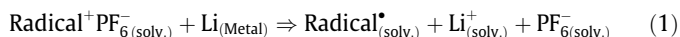


Fig. 1. (a) Spin-up density for radical TEMPO, (b) PTMA = TEMPO radical linked to the PMMA backbone, (c) redox processes for the nitroxide center.

The Li-ion PTMA battery is made of a metallic lithium anode and of a radical polymer at the cathode. The two electrodes are immersed in an electrolyte solvent, usually an aprotic polar solvent containing an electrolyte salt such as LiPF_6 . In Ref. [7], it was shown that the full discharge reaction of the Li-ion PTMA radical battery can be expressed as:



where Radical stands for the active pendant group of the polymer (e.g. TEMPO for PTMA) and the superscript dot symbolizes the unpaired electron. The OCV for this reaction (1), also called the redox potential E_{redox} , is the reduction potential of the couple (Radical⁺/Radical[•]) relative to the couple (Li⁺/Li): $E_{\text{vs Li/Li}^+}(\text{Radical}^+/\text{Radical}^{\bullet})$. At the anode, the lithium is oxidized while, at the cathode, a reduction of the oxidized PTMA⁺ occurs.

The full redox potential is then obtained from the absolute reduction potential E_{abs} for both half-reactions as: $E_{\text{redox}} = E_{\text{abs}}(\text{Radical}^+/\text{Radical}^{\bullet}) - E_{\text{abs}}(\text{Li}^+/\text{Li})$. E_{abs} is directly linked to the Gibbs free energy change ΔG (J/mol) with $E_{\text{abs}} = -\Delta G/(nF)$ where n is the number of electrons involved in the reaction and F is the Faraday constant (C/mol). For the reduction at the radical cathode, the Gibbs free energy change ΔG per molecule is approximated by the total electronic energy change ΔE_{tot} between the oxidized and reduced relaxed states, e.g. the adiabatic ionisation. The simulations are performed using the GAUSSIAN 09 code [12] which implements the SMD (Solvation Model Density) polarized continuum model [10] allowing to compute the solvation free energy for any type of solvent. This ΔSCF method can then be summarized as:

$$E_{\text{abs}}(\text{Radical}^+/\text{Radical}^{\bullet}) = \frac{-\Delta G^0}{nF} \approx - \underbrace{\left(E_{\text{tot}}^{\text{Radical}^{\bullet}} - E_{\text{tot}}^{\text{Radical}^+} \right)}_{\text{B3LYP/6-31+G}^* \text{ SMD}} \quad (2)$$

where the B3LYP [13,14] hybrid functional is used with the 6-31+G* Pople basis set. For the computation of the absolute reduction potential of the anode $E_{\text{abs}}(\text{Li}^+/\text{Li})$ in a solvent, we refer the reader to Ref. [7]. In our simulations, ethylene carbonate is used as solvent taking the SMD parameters from Ref. [15]. For the anode, we computed a $E_{\text{abs}}(\text{Li}^+/\text{Li})$ of 1.29 V.

The main goal of this work is to compute the voltage of theoretical Li-ion organic batteries. Starting from the TEMPO molecule, newly designed molecules are built by substituting the four methyl groups around the nitroxide center with various functional groups. We arbitrarily use $-\text{OCH}_3$ as an electron donating group (EDG) as well as various electron-withdrawing groups (EWGs): $-\text{H}$,

$-\text{CH}_2\text{OH}$, $-\text{CH}_2\text{Br}$, $-\text{CBr}_3$, $-\text{CH}_2\text{Cl}$, $-\text{CCl}_3$, $-\text{NO}_2$, $-\text{CH}_2\text{F}$, $-\text{CHF}_2$, $-\text{CF}_3$ and $-\text{F}$. Since the reference is the methyl group, the $-\text{H}$ and $-\text{CH}_2\text{OH}$ groups are in this case attached to the EDGs category. In Fig. 2a, the four possible positions of the methyl groups are named A, B, C and D. Since the PTMA polymer is modeled with the simpler TEMPO radical, these four positions present a mirror symmetry as illustrated in Fig. 2b. Position A is equivalent to position D and B is equivalent to C. On the other hand, position A is not equivalent to position B (or D to C). A and D positions are closer to each other than positions B and C. Consequently the influence of the functional groups will be different at A and D than at the B and C positions. This mirror symmetry allows to reduce the number of simulations since, for example, the substitution of two methyl groups at positions A and B is equivalent to that at positions C and D (written CD in the following). For a given functional group, 9 newly designed molecules are investigated with substitutions at the following positions: A, B, AB (equivalent to CD), AC (equivalent to BD), AD, BC, ABC (equivalent to BCD), ABD (equivalent to ACD) and ABCD. In Fig. 2c, the substitutions of the methyl groups by trifluoromethyl groups (CF_3) are illustrated: from top to bottom, one CF_3 at position A, two CF_3 at AD, three CF_3 at ABC and four CF_3 at ABCD. The geometry of every new molecule created by substitution of functional groups is optimized with the same level of theory as mentioned above. Note that conformational searches are not explicitly performed assuming that variations of the computed voltages between various rotamers are small. Indeed, the reduction potential being computed as a difference between $E_{\text{tot}}^{\text{Radical}^{\bullet}} - E_{\text{tot}}^{\text{Radical}^+}$, the changes in total energies from one conformer to another are expected to be partially canceled.

3. Results and discussion

In Table 1, the computed voltages of the newly designed radicals are listed. They are to be compared with the 3.6 V of the Li-ion PTMA battery which is simulated for the TEMPO radical within our model system. In principle, only differences with respect to that reference are meaningful. However, given the excellent agreement with the experimental value (3.56 V), we chose to present them on an absolute scale. For example, in the case of the strong electron-withdrawing groups $-\text{CF}_3$, the voltage is computed to be 4.10 V for a substitution at position A and at 3.96 V at position B. The inductive effect of the EWGs tends to attract and stabilize the unpaired electron localized on the nitroxide center which makes the oxidation of the molecule harder, thus increasing in the redox potential. When all four methyl groups are replaced by trifluoromethyl groups, our simulation shows a voltage reaching 5.40 V. With $-\text{NO}_2$, the strongest EWG considered here, the voltage reaches 6.24 V with four substitutions. As expected, the general trend is that the stronger the EWG, the higher the voltage. The effect of the $-\text{OCH}_3$ EDG (more electron-donor than a methyl group) induces a more erratic variation. With a functional group at position A, the voltage increases to 3.71 V whereas the voltage is only at 3.59 V when the substitution occurs at position B. With two substitutions, the voltage can vary from 3.40 to 3.87 depending on the choice of the positions. With a full replacement of the four methyl groups, the voltage decreases but only to 3.50 V. The lowest computed voltage among all functional groups occurs at 3.39 V with the $-\text{CH}_2\text{OH}$ groups with two substitutions at position A and C. On the other hand, the same group but with four substitutions gives an increase in the voltage at 3.93 V.

To investigate further these different behaviors, the variation of the voltage was analyzed as a function of the atomic partial charges (APT [16]) on the nitroxide center (NO) and as a function of the HOMO energy levels, as illustrated in Fig. 3 for the $-\text{OCH}_3$ and $-\text{CF}_3$ groups (similar graphs for all the functional groups can

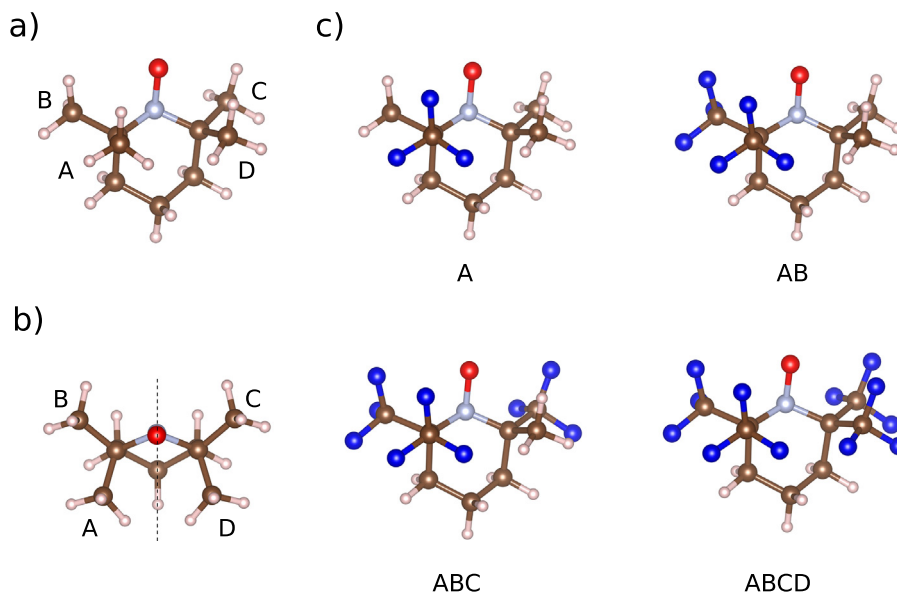


Fig. 2. (a) TEMPO molecule with the four positions (A, B, C and D) of the methyl groups around the nitroxide center. (b) Top view of the TEMPO radical illustrating the mirror symmetry. (c) Illustration of the substitution of the methyl groups by trifluoromethyl groups: one CF₃ at position A, two CF₃ at AB, three CF₃ at ABC and four CF₃ at ABCD, respectively.

Table 1

Computed voltages for the newly designed radicals: the TEMPO radical modified with functional groups at all the possible positions. These voltages are computed for a Li-ion battery in ethylene carbonate as solvent. These values are to be compared to the 3.6 V of the Li-ion PTMA battery. The averaged voltages for a given number of substitutions for each functional group are listed in the Avg(# of substitution) lines.

Position	Functional groups											
	OCH ₃	H	CH ₂ OH	CH ₂ F	CH ₂ Cl	CH ₂ Br	CHF ₂	CBr ₃	CCl ₃	CF ₃	NO ₂	F
A	3.71	3.48	3.65	3.82	3.84	3.85	4.00	4.08	4.10	4.09	4.26	4.10
B	3.59	3.63	3.82	3.75	3.78	3.78	3.96	4.05	4.06	4.06	4.29	3.96
Avg(1)	3.65	3.56	3.74	3.79	3.81	3.81	3.98	4.07	4.08	4.07	4.28	4.03
AB (CD)	3.40	3.59	3.76	4.00	4.04	4.06	4.37	4.48	4.54	4.56	4.97	4.44
AC (BD)	3.87	3.47	3.39	4.03	4.01	4.05	4.38	4.59	4.60	4.63	5.00	4.65
AD	3.61	3.69	4.04	3.98	4.01	4.03	4.35	4.44	4.51	4.58	5.01	4.34
BC	3.73	3.56	3.84	4.05	4.07	4.10	4.38	4.60	4.61	4.60	5.02	4.48
Avg(2)	3.64	3.56	3.70	4.01	4.03	4.06	4.37	4.53	4.57	4.59	4.99	4.50
ABC (BCD)	3.47	3.58	4.07	4.22	4.31	4.38	4.77	5.00	5.06	5.12	5.68	5.02
ABD (ACD)	3.41	3.66	3.93	4.22	4.28	4.34	4.76	4.91	4.99	5.09	5.70	4.84
Avg(3)	3.44	3.62	4.00	4.22	4.29	4.36	4.77	4.95	5.02	5.10	5.69	4.93
ABCD	3.50	3.69	3.93	4.43	4.56	4.63	5.14	5.36	5.43	5.63	6.24	5.40

be found in the [supplementary information](#)). For the $-\text{CF}_3$ group, the decrease in the negative charge on the NO center is due to its strong electron-withdrawing character. It is directly correlated with the increase in the voltage (bottom left in Fig. 3). The same kind of correlation is found between the voltage and the HOMO levels of the modified compounds (bottom right in Fig. 3) where an increase in the voltage is linked to the decrease in energy of the HOMO levels. In contrast, for the $-\text{OCH}_3$ group, neither the APT charges nor the HOMO levels are correlated to the variation of the voltage as shown in the top graphs of Fig. 3. Moreover, this EDG can induce lower voltages despite a decrease in energy of the HOMO levels. This shows that the variation of the reduction potential cannot be only ascribed only to the electron-withdrawing/donating effects. Various phenomena can result in changes to the redox properties [17] and a full analysis of these effects is beyond the scope of this work.

The present theoretical approach does not allow to predict whether or not the newly designed molecules can be synthesized. Furthermore, it is also difficult to assess in advance whether they

can lead to a working battery (for example, in terms of the stability with respect to the solvent when used with such high redox potentials or in terms of the transfer rate).

The position of the substitutions being hard to control when synthesizing the molecules, the averaged voltages are computed for given a number of substitutions for each functional group, as reported in Table 1. In Fig. 4, these values are plotted according the capacity of the theoretical battery. To calculate the capacity, the molar mass of the PMMA is added to the molecular weight of the modified radical in order to compare them to the actual PTMA. Fig. 4 shows a voltage range between 3.4 and 6.2 V. But these increases in the potential sometimes induce a huge drop in the capacity due the high molecular weight of some radicals. A good compromise between the tuning of the voltage and the loss in capacity can be achieved with the functional group $-\text{NO}_2$ or the simpler Fluor atom. Our work shows that ab initio techniques can be used to design new organic cathodes. This paves the way for a systematic development of low-cost and high performance batteries.

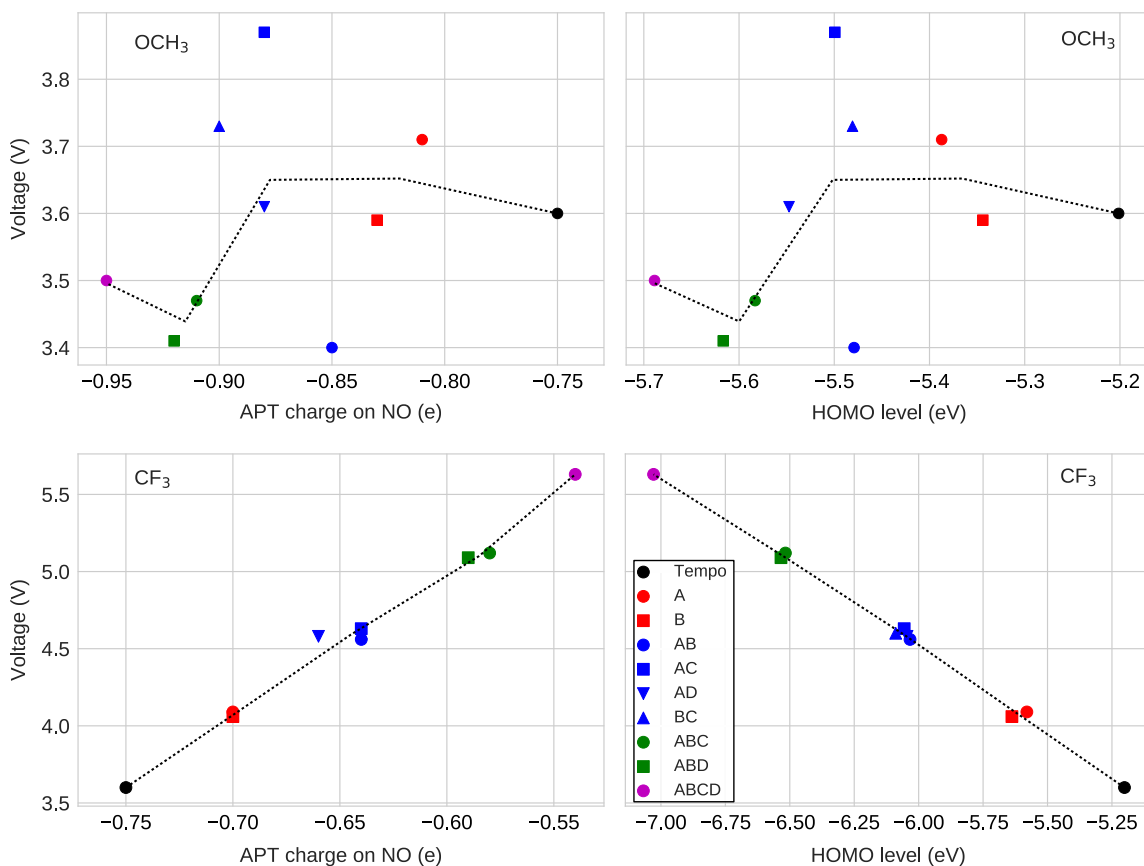


Fig. 3. Voltages (vs. Li^+/Li) as a function of the APT charges on the nitroxide center (NO) and as a function the HOMO levels for two typical examples of newly designed radicals. Top: modified TEMPO radicals with the $-\text{OCH}_3$ group. Bottom: modified TEMPO radicals with the $-\text{CF}_3$ group. The colors indicate the number of substitutions (1 in red, 2 in blue, 3 in green, and 4 in purple). For each color, the symbols refer to the positions of the substitutions as indicated in the legend using the same letters as in Table 1. The black dotted line connects the average values for the different positions at a given a number of substitutions. (For interpretation of the references to color in this figure legend, the reader is referred to the web version of this article.)

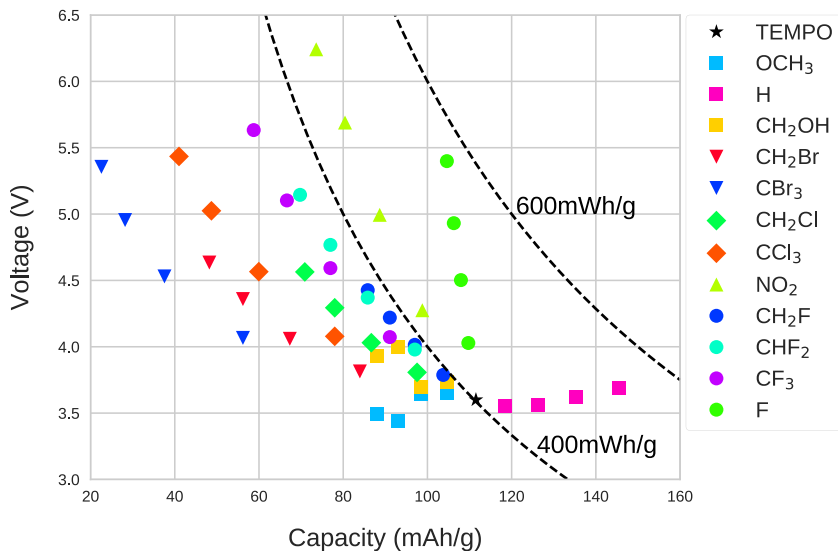


Fig. 4. Voltage (vs. Li^+/Li) versus capacity for the newly designed radicals (modified TEMPO radicals). The capacity is calculated by adding the molecular weight of PMMA to allow the comparison with the PTMA (TEMPO attached to PMMA). These values are to be compared to the 3.6 V and the 111 mAh/g of the Li-ion PTMA battery (indicated by the black star TEMPO). This graph is to be read as follows: for a functional group listed in the legend, the nearest, second nearest, third nearest and the farthest values to the TEMPO black star correspond to one, two, three and four substitutions respectively.

4. Conclusion

Based on a previously tested Δ SCF technique, we predicted the shift in reduction potentials when substituting the methyl group of the TEMPO radical with various functional groups. These theoretically designed radicals exhibit a range in voltage from 3.4 up to 6.2 V allowing for a potential fine-tuning depending on specific need for various battery applications.

Acknowledgement

We thank Prof. Xavier Blase for his helpful support. The authors acknowledge the National Fund for Scientific Research [F.R.S.-FNRS] of Belgium for financial support. N.D., J.-F.G. and G.-M.R. acknowledge support from the Communauté française de Belgique through the BATTAB project (ARC 14/19-057). This research is connected to the BATWAL project sponsored by the Region Wallone. Computational resources were provided by the supercomputing facilities of the Université catholique de Louvain (CISM/UCL) and the Consortium des Equipements de Calcul Intensif en Fédération Wallonie-Bruxelles (CECI).

Appendix A. Supplementary material

Supplementary data associated with this article can be found, in the online version, at <https://doi.org/10.1016/j.commat.2017.10.038>.

References

- [1] J.-M. Tarascon, M. Armand, Issues and challenges facing rechargeable lithium batteries, *Nature* 414 (6861) (2001) 359–367, <https://doi.org/10.1038/35104644>. <<http://www.nature.com/nature/journal/v414/n6861/abs/414359a0.html>> .
- [2] P. Poizot, F. Dolhem, Clean energy new deal for a sustainable world: from non-CO₂ generating energy sources to greener electrochemical storage devices, *Energy Environ. Sci.* 4 (6) (2011) 2003–2019, <https://doi.org/10.1039/C0EE00731E>. <<http://pubs.rsc.org/en/content/articlelanding/2011/ee/c0ee00731e>> .
- [3] Y. Liang, Z. Tao, J. Chen, Organic electrode materials for rechargeable lithium batteries, *Adv. Energy Mater.* 2 (7) (2012) 742–769, <https://doi.org/10.1002/aenm.201100795>. <<http://onlinelibrary.wiley.com/doi/10.1002/aenm.201100795/abstract>> .
- [4] Z. Song, H. Zhou, Towards sustainable and versatile energy storage devices: an overview of organic electrode materials, *Energy Environ. Sci.* 6 (8) (2013) 2280–2301, <https://doi.org/10.1039/C3EE40709H>. <<http://pubs.rsc.org/en/content/articlelanding/2013/ee/c3ee40709h>> .
- [5] T. Janoschka, M. Hager, U. Schubert, Powering up the future: radical polymers for battery applications, *Adv. Mater.* 24 (48) (2012) 6397–6409, <https://doi.org/10.1002/adma.201203119>.
- [6] S. Muench, A. Wild, C. Friebe, B. Hupler, T. Janoschka, U.S. Schubert, Polymer-based organic batteries, *Chem. Rev.* 116 (16) (2016) 9438–9484, <https://doi.org/10.1021/acs.chemrev.6b00070>, PMID: 27479607.
- [7] N. Dardenne, X. Blase, G. Hautier, J.-C. Charlier, G.-M. Rignanese, Ab initio calculations of open-cell voltage in Li-ion organic radical batteries, *J. Phys. Chem. C* 119 (41) (2015) 23373–23378, <https://doi.org/10.1021/acs.jpcc.5b07886>.
- [8] W. Kohn, L.J. Sham, Self-consistent equations including exchange and correlation effects, *Phys. Rev.* 140 (1965) A1133–A1138.
- [9] P. Hohenberg, W. Kohn, Inhomogeneous electron gas, *Phys. Rev.* 136 (1964) B864–B871.
- [10] A.V. Marenich, C.J. Cramer, D.G. Truhlar, Universal solvation model based on solute electron density and on a continuum model of the solvent defined by the bulk dielectric constant and atomic surface tensions, *J. Phys. Chem. B* 113 (18) (2009) 6378–6396, <https://doi.org/10.1021/jp810292n>.
- [11] K. Nakahara, S. Iwasa, M. Satoh, Y. Morioka, J. Iriyama, M. Suguro, E. Hasegawa, Rechargeable batteries with organic radical cathodes, *Chem. Phys. Lett.* 359 (56) (2002) 351–354, [https://doi.org/10.1016/S0009-2614\(02\)00705-4](https://doi.org/10.1016/S0009-2614(02)00705-4). <<http://www.sciencedirect.com/science/article/pii/S0009261402007054>> .
- [12] M.J. Frisch, G.W. Trucks, H.B. Schlegel, G.E. Scuseria, M.A. Robb, J.R. Cheeseman, G. Scalmani, V. Barone, B. Mennucci, G.A. Petersson, H. Nakatsuji, M. Caricato, X. Li, H.P. Hratchian, A.F. Izmaylov, J. Bloino, G. Zheng, J.L. Sonnenberg, M. Hada, M. Ehara, K. Toyota, R. Fukuda, J. Hasegawa, M. Ishida, T. Nakajima, Y. Honda, O. Kitao, H. Nakai, T. Vreven, J.A. Montgomery, Jr., J.E. Peralta, F. Ogliaro, M. Bearpark, J.J. Heyd, E. Brothers, K.N. Kudin, V.N. Staroverov, R. Kobayashi, J. Normand, K. Raghavachari, A. Rendell, J.C. Burant, S.S. Iyengar, J. Tomasi, M. Cossi, N. Rega, J.M. Millam, M. Klene, J.E. Knox, J.B. Cross, V. Bakken, C. Adamo, J. Jaramillo, R. Gomperts, R.E. Stratmann, O. Yazyev, A.J. Austin, R. Cammi, C. Pomelli, J.W. Ochterski, R.L. Martin, K. Morokuma, V.G. Zakrzewski, G.A. Voth, P. Salvador, J.J. Dannenberg, S. Dapprich, A.D. Daniels, Farkas, J.B. Foresman, J. V. Ortiz, J. Cioslowski, D.J. Fox, Gaussian09 Revision D.01, Gaussian Inc. Wallingfor.
- [13] K. Kim, K.D. Jordan, Comparison of density functional and MP2 calculations on the water monomer and dimer, *J. Phys. Chem.* 98 (40) (1994) 10089–10094, <https://doi.org/10.1021/j100091a024>.
- [14] P.J. Stephens, F.J. Devlin, C.F. Chabalowski, M.J. Frisch, Ab initio calculation of vibrational absorption and circular dichroism spectra using density functional force fields, *J. Phys. Chem.* 98 (45) (1994) 11623–11627, <https://doi.org/10.1021/j100096a001>.
- [15] S.E. Burkhardt, J. Bois, J.-M. Tarascon, R.G. Hennig, H.D. Abruja, Li-carboxylate anode structure-property relationships from molecular modeling, *Chem. Mater.* 25 (2) (2013) 132–141.
- [16] J. Cioslowski, A new population analysis based on atomic polar tensors, *J. Am. Chem. Soc.* 111 (22) (1989) 8333–8336, <https://doi.org/10.1021/ja00204a001>.
- [17] G. Grynova, M.L. Coote, Origin and scope of long-range stabilizing interactions and associated SOMO-HOMO conversion in distonic radical anions, *J. Am. Chem. Soc.* 135 (41) (2013) 15392–15403, <https://doi.org/10.1021/ja404279f>.